A Modified Chicken Swarm Optimisation Algorithm for Feature Selection of a Multi-Textural Feature Digital Image Classification System

[1]Agboola F. Fadeke; [2]Ismaila W. Oladimeji; [3]Omotosho I. O; [4]Falohun S. Adeleye; [5]Ismaila Folasade M.

[1] Department of Computer Science, Modibbo Adama University, Nigeria
[2] Department of Computer Science, Ladoke Akintola University of Technology, Nigeria
[3] Department of Cybersecurity Science, Ladoke Akintola University of Technology, Nigeria
[4] Department of Computer Engineering, Ladoke Akintola University of Technology, Nigeria
[5] Department of Computer Science, Fountain University, Osogbo, Nigeria

orcid.org/0000-0002-6390-4715

Publication Date: 2025/04/19

Abstract: Digital image processing is a process that involves analyzing and manipulating images digitally via computer which has various applications such as remote sensing, surveillance, Biometrics, Medical field and more. Brain tumours are diseases that occur in the brain when abnormal cells begin to develop in an uncontrolled manner. The growth could be fatal and deadly if the accumulation continues. Thus, the quick discovery of the brain tumour is significant and helpful for further investigation. Classification and identification are challenging due to image complexity and unclear causes. This paper proposes a modified Chicken Swarm Optimisation (mCSO) technique for feature selection in digital images classification. 1800 brain MRI images was acquired from the Kaggle database. The brain tumour dataset were preprocessed. Three techniques (gray-level co-occurrence matrix, discrete wavelet transformation, and Gabor filter) were used for feature extraction and their outputs were fused by Serial Sum technique. The Chicken Swarm Optimisation was modified by Simulated Binary Crossover to prevent its local optima problem. The result of the analysis is focused on multi-binary classification to determine the efficacy of fusing feature extraction methods. The study found that the technique with mCSO achieved an accuracy of 97.61% better than the standard Chicken Swarm Optimisation technique that achieved accuracy of 96.50%.

Keywords*: *Chicken Swarm Optimisation, Gray-Level Co-Occurrence Matrix, Discrete Wavelet Transformation, Gabor Filter, Simulated Binary Crossover, Serial Sum.

How to Cite: Agboola F. Fadeke, Ismaila W. Oladimeji, Omotosho I. O. Falohun S. Adeleye, Ismaila Folasade M. (2025) A Modified Chicken Swarm Optimisation Algorithm for Feature Selection of a Multi-Textural Feature Digital Image Classification System. *International Journal of Innovative Science and Research Technology,* 10(3), 3213-3226. https://doi.org/10.38124/ijisrt/25mar2010

I. INTRODUCTION

Digital Image Processing is a process that involves analyzing and manipulating images digitally via computer to make them more informative for human interpretation and picture information for tasks such as maintaining storage, fast transmission, and extraction of pictorial data. It is a use of computer algorithms, in order to get enhanced image or to extract some useful information. It has various applications such as Image enhancement, automatic inspection, remote sensing, surveillance, Biometrics, Medical field and more. Image processing provides a lot of

ISSN No:-2456-2165 https://doi.org/10.38124/ijisrt/25mar2010

help in the medical field and is used widely in the following things: Gamma-ray imaging, Positron Emission Tomography scan, X-Ray imaging, Medical Computer Tomography, Ultraviolet radiation imaging, and so on. Medical CT scan helps to scan cancer, fractures, Heart diseases, kidney stones, Brain tumours, etc. [1], [24]. .

Brain tumour detection systems undergo five stages which include image accumulation, image preprocessing, image feature extraction and image classification. However, image features extraction is a crucial step in machine learning which as to do with selecting and transforming raw data into relevant, informative and discriminative features for model building. Some of the machine learning techniques employed for feature extraction are gray-level co-occurrence matrix (GLCM), discrete wavelet transformation (DWT), Principal Component Analysis, Local Binary Pattern [3] [4], Gabor wavelet [5] Gradient Local Binary Pattern [2] etc. And some extracted features were fused like DWT, Gabor wavelet and GLCM by Mathew *et al*. (2017), DWT and Gabor filter by authors in [7] etc.

However, the use of feature extraction techniques suffer from redundant features, high dimensionality, which eventually produce low accuracy. Hence the extracted features are further subjected to feature selection. Feature selection is the processing of selecting a subset of relevant features to improve model performance. Some of the techniques are Genetic algorithm [8], Chicken Swarm Optimisation (CSO) [9], bee swarm optimization, [10]. CSO is a new bio-inspired algorithm developed by [11]. The CSO algorithm has excellent research potential because of its good convergence speed, robust to parameter settings and noise and has high accuracy. CSO can efficiently extract the chickens' swarm intelligence to optimize problems; [12]. CSO falls into optimal local conditions easily and has a premature convergence problem. When used in high-dimensional space, although roosters have a minimal number, they play guiding roles in the whole population, and the hens have the maximum quantity, but they do not provide feedback to roosters. This makes the algorithm rapidly fall into an optimal local solution when roosters sink into local minima [13]. To address these limitations, it is essential to effectively extract the characteristics of the most discriminative images to increase the efficiency and accuracy of a CAD system [14].

II. RELATED WORK

Numerous researchers have investigated various classification strategies, both supervised and unsupervised, to enhance the accuracy of brain tumour picture classifications. The authors in {15] presented a neural network-based method for the detection and classification of brain tumours. This technique emphasizes the segmentation of various brain regions, encompassing white matter (WM), grey matter (GM), cerebrospinal fluid (CSF), and the cancer region. The segmentation method assesses the quality rate for each region separately. A neural network-based classifier is employed for classification, attaining an accuracy of 83%, underscoring the method's efficacy in accurately recognizing and categorising brain tumours.

In 2017, the researchers in [16] enhanced the categorisation of brain tumours by incorporating contemporary mathematical modelling and intelligence technologies. Their review showed how important automatic segmentation is and how support vector machines are better at accurately classifying brain tumours than artificial neural networks. The results of this study laid the groundwork for more research into feature selection methods in brain tumours, showing the need for complex algorithms that can handle large amounts of data. In 2017, the authors in [6] presented a method for classifying brain tumours from MRI images via support vector machines (SVM). Otsu's thresholding served as the photos' preprocessing, and the K-means clustering algorithm detected tumours after that. A hybrid method integrating DWT, Gabor wavelet, and GLCM was utilised for feature extraction. Of the SVM approaches evaluated—linear kernel, polynomial kernel, and RBF kernel—the linear kernel had the greatest accuracy, at roughly 72%. The researchers in [17] proposed a technique for the multi-class classification of brain MRI images. Feature extraction was conducted with Discrete Wavelet Transform (DWT) and Principal Component Analysis, which provided the input data for the classification network. The Random Forest algorithm was subsequently employed, attaining the greatest accuracy of 95.7% in the classification of various brain disorders. The authors in [18] employed the Adaboost classifier to proficiently categorise brain tumours. The first step in the classification process was to get texture features from MRI images using the Grey Level Co-occurrence Matrix (GLCM) method, which shows where there are strong spatial correlations in the image data. Twenty-two unique features were retrieved to create a comprehensive dataset for classification. When the Adaboost algorithm was used, the classification accuracy went up to a high point of 89.90%, showing that the method is good at telling the difference between different types of brain tumours. Also, in 2018, the writers in [8] proposed a sophisticated technique for brain tumour segmentation and classification, with the objective of enhancing accuracy and reliability in tumour detection. The procedure began with a lengthy preprocessing phase that included manually removing non-brain tissues from the skull. This was followed by an advanced thresholding technique that improved the quality of the images and highlighted the locations of the tumours. Subsequent to preprocessing, a genetic algorithm was utilised to effectively identify the most pertinent features from an extensive dataset, hence enhancing the classification process. The concluding phase entailed the

ISSN No:-2456-2165 https://doi.org/10.38124/ijisrt/25mar2010

use of the Support Vector Machine algorithm for tumour classification, yielding a classification accuracy of 90%, thus demonstrating the efficacy of this multi-step methodology in precisely identifying brain tumours.

Authors in [19] devised a technique employing a regularised extreme learning machine to categorise MRI scans as benign or malignant. Their methodology utilised a hybrid PCA-based normalised GIST technique for feature extraction, resulting in an improved classification accuracy of roughly 94.23%. The advent of chaotic chicken swarm optimisation (CCSO) by [20] signified a crucial development in feature selection techniques. Their technique addressed the problem of local minima, a prevalent obstacle in conventional evolutionary algorithms, thereby improving the search for optimal features. This novel method demonstrated superior performance compared to many established algorithms, signifying a substantial advancement in the pursuit of efficient feature selection for cancer classification.

In 2020, [21] proposed a modified chicken swarm optimisation technique specifically designed for feature selection in brain tumour classification systems. This advancement signifies the continuous progression of swarm intelligence methodologies and their utilisation in medical imaging and classification endeavours. Also in 2021, [22] investigated diverse feature selection strategies to improve the accuracy of lung cancer categorisation. Their research highlighted the significance of eliminating superfluous information to enhance classification efficacy, a premise that aligns with the goals of numerous modern algorithms.

III. MATERIALS AND METHODS

This section presents the materials, the source of the brain MR image dataset, and the algorithm used to perform brain MR tissue segmentation. Figure 1 shows the flow process of the work, where the proposed system is divided into six parts: (A) image preprocessing (B) segmentation using fuzzy c-means (C) fusion of Gabor, DWT, and GLCM (D) modified CSO optimisation for feature selection (E) classification using SVM. The MRI brain tumour images were downloaded from the Kaggle database. A total of 1800 images is used for classification. Where the tumour images are 1420 and the non-tumour images are 380.

➢ *Data Pre-Processing*

A series of pre-processing steps were applied to improve the image quality for further processing. The acquired images were passed through different pre-processing techniques, and the MRI brain images were resized to equal pixels and converted to a grey-level image. Additionally, due to various factors like faulty switching and environmental conditions, impulse noise affects the majority of MRI images. Hence, the images were filtered. Filtering in image processing is the main function used to accomplish interpolation, noise reduction, and resampling.

A combination of mean and median filters for different pixel values was used to eliminate the noise in MRI images in this study. The image details at the edge are preserved using a median filter while removing noise. It works by going through the images pixel by pixel and replacing each with the median value of the neighbouring pixel.

Due to the intra-scan and inter-scan image intensity variations, MR image intensity normalisation is required after detecting slices that include tumours. Image intensity normalisation is necessary for quantitative texture analysis. In this study, the histogram normalisation method was applied before quantitative texture analysis, stretching and shifting the original image histogram to include all the grayscale levels in the image. It is defined as shown in Equation 1.

$$f(x,y) = \frac{I_{min}-I_{max}}{h_{max}-h_{min}}(h(x,y)-h_{min})+I_{max} \quad (1)$$

Where $h(x,y)$is the original histogram of the initial image, $f(x,y)$ is the new histogram, and $h_{min}$and $h_{max}$are the smallest and largest gray scale level, respectively. I_{min} and I_{max} are the new minimum and new maximum intensity levels. Figures 2 illustrate the pre-processing stages. The acquired images were passed through different pre-processing techniques, and the MRI brain images were resized to equal pixels and converted to a grey-level image. And then, Fuzzy C-Means (FCM) for segmentation. The steps involved in fuzzy c-means image segmentation are depicted in the algorithm below;

- *Initialize the cluster centers c_i and t = 0.*

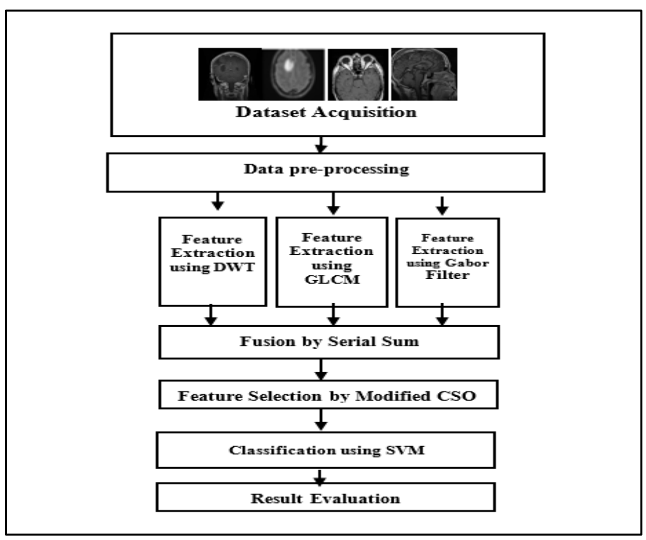

Fig 1 The Work flow diagram of the developed Bain Tumour Classification System

ISSN No:-2456-2165 https://doi.org/10.38124/ijisrt/25mar2010

- *Initialize the fuzzy partition memberships functions μ_{ij} according to equation (2)*

$$\mu_{ij} = \left(\sum_{m=1}^{C} \left(\frac{\|x_j - c_i\|}{\left(\|x_j - c_m\|\right)^{2/(k-1)}} \right) \right)^{-1} \qquad (2)$$

- *Let $= t + 1$ and compute new cluster centres c_i using equation (3).*

$$c_i = \frac{\sum_{j=1}^{N} \mu_{ij}^{k} x_j}{\sum_{j=1}^{N} \mu_{ij}^{k}} \qquad (3)$$

- *Repeat Steps 2 to 3 until convergence is noticed.*

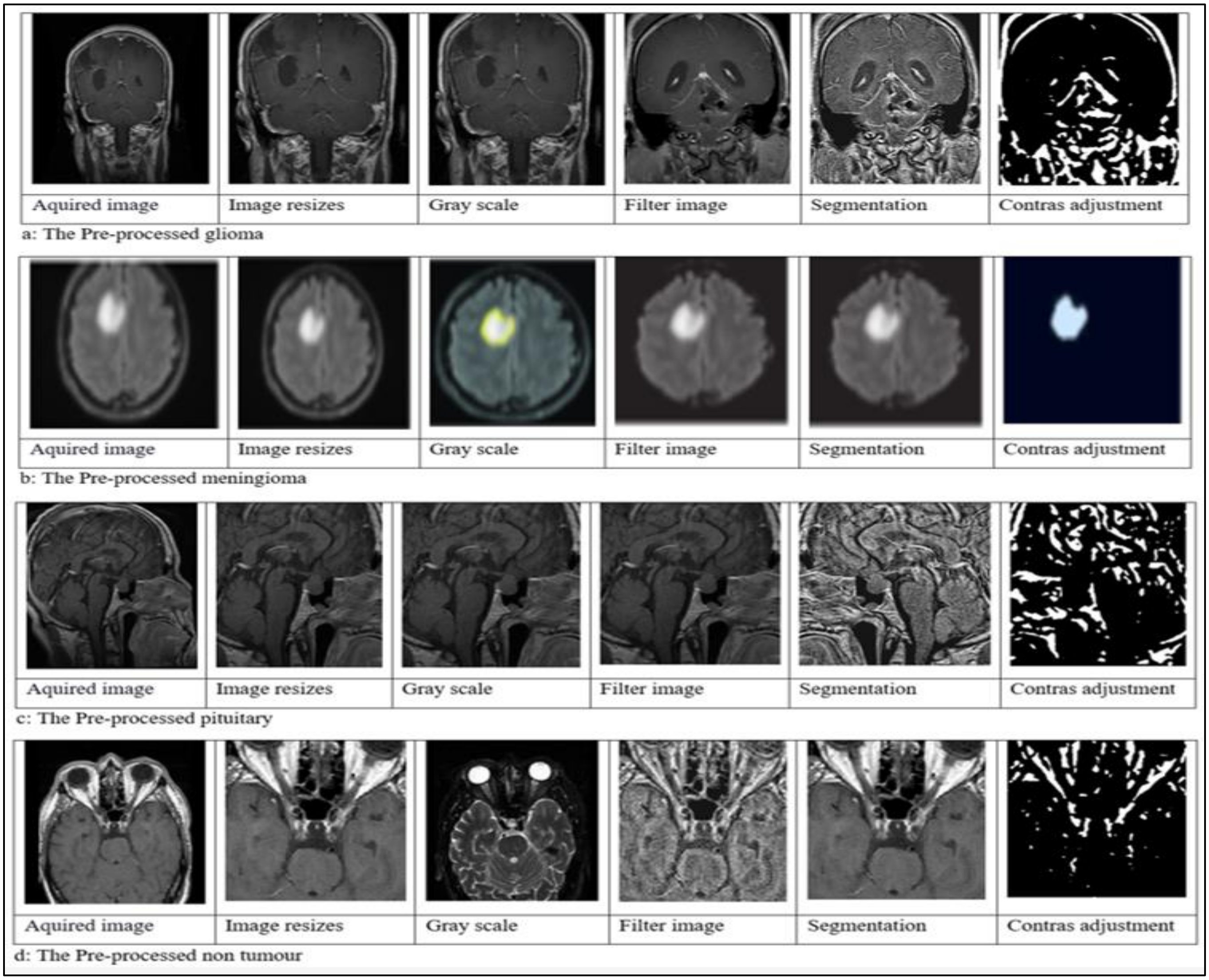

Fig 2 The Pre-Processing Images of the Brain Tumour and Non Tumour

➢ *Feature Extraction*

The feature extraction process helps to represent the target object in its precise and unique form of single values or matrix vector. For this reason, the combination of Gabor filter, DWT, and GLCM produces the six values features that contain the statistical information of the detected brain tumour image.

- *Feature extraction using Gabor filter*

Hungarian-born electrical engineer Dennis Gabor developed a Gabor wavelet in 1946. It was created from one particular atom by dilation and rotation in a two-dimensional case and provides a complete image representation [33]. Nowadays, Gabor functions are frequently used for feature extraction, especially in texture-based image analysis (such as classification, segmentation, or edge detection) and, more practically, pattern recognition [27, 28, 34, 35,36,37]. The pseudocode of Gabor filter is shown in Algorithm 1.

ISSN No:-2456-2165 https://doi.org/10.38124/ijisrt/25mar2010

Algorithm 1 Pseudocode of Gabor filter [27,28].

```
For each frequency f in the frequency list flist:
 For each orientation ϕ in the orientation list olist:
    Construct a Gabor filter g(f, ϕ),
    Convolve g(f, ϕ) with original image I, get response
    image R,
    Compute the mean response in R, denote as r,
    Count # of pixels Nr that have a larger value than r,
    Divide R into n x m frames,
    For i = 1 to n:
      For j = 1 to m:
        Count the # of strong responses N_i,j and
        compute the ratio r:
        r =N_i,j / Nr;
        Append r to the feature vector x:
Finally, x=[r1,r2,…r|flist|*|olist|*n*m].
```

- *Feature extraction using DWT*

The authors in [38] described the discrete wavelet transform (DWT) as a mathematical tool for analysing time series. The DWT provides an efficient feature extraction result by performing the multi-level decomposition of the image [39,40]. Therefore, in this work, three levels of 2-D DWT decomposition to reduce the image matrix size using the "Daubechies" filter was implemented [25, 26]. The pseudocode of DWT is shown in Algorithm 2.

Algorithm 2 Pseudocode of DWT [28,29].

Input: $I_{m\times m} = \{m \times m\} \in R^2$
Output: Labels (AD, MCI, HC)
Wavelet Decomposition:
$[LL\,1_{m/2\times m/2}, LH\,1_{m/2\times v}, HL\,1_{m/2\times m/2}, HH\,1_{m/2\times m/2}] = 2\,D\_DWT\,(I_{m\times m})$
$[LL\,2_{m/4\times m/4}, LH\,2_{m/4\times m/4}, HL\,2_{m/4\times m/4}, HH\,2_{m/4\times m/4}] = 2D_{DWT}\,(LL\,1_{m/4\times m/4})$
Reshape sub-bands and remove zeros:
$LH\,1_v = \text{Reshape}(LH\,1, [m/2 \times m/2, 1])\&\text{Remove}(\text{zeros})$
$HL\,1_v = \text{Reshape}(HL\,1, [m/2 \times m/2, 1])\&\text{Remove}(\text{zeros})$
$HH\,1_v = \text{Reshape}(HH\,1, [m/2 \times m/2, 1])\&\text{Remove}(\text{zeros})$
$LL\,2_v = \text{Reshape}(LL_2, [m/4 \times m/4, 1])\&\text{Remove}(\text{zeros})$
$LH\,2_v = \text{Reshape}(LH\,2, [m/4 \times m/4, 1])\&\text{Remove}(\text{zeros})$
$HL\,2_v = \text{Reshape}(HL\,2, [m/4 \times m/4, 1])\&\text{Remove}(\text{zeros})$
$HH\,2_v = \text{Reshape}(HH\,2, [m/4 \times m/4, 1])\&\text{Remove}(\text{zeros})$
Feature Extraction:
$(f_1^{(1)}, f_2^{(1)}, f_3^{(1)}, f_4^{(1)}, f_5^{(1)}, f_6^{(1)}, f_7^{(1)}) = TD\_PSD(LH\,1_v)$
$(f_1^{(2)}, f_2^{(2)}, f_3^{(2)}, f_4^{(2)}, f_5^{(2)}, f_6^{(2)}, f_7^{(2)}) = TD\_PSD(HL\,1_v)$
$(f_1^{(3)}, f_2^{(3)}, f_3^{(3)}, f_4^{(3)}, f_5^{(3)}, f_6^{(3)}, f_7^{(3)}) = TD\_PSD(HH\,1_v)$
$(f_1^{(4)}, f_2^{(4)}, f_3^{(4)}, f_4^{(4)}, f_5^{(4)}, f_6^{(4)}, f_7^{(4)}) = TD\_PSD(LL\,2_v)$
$(f_1^{(5)}, f_2^{(5)}, f_3^{(5)}, f_4^{(5)}, f_5^{(5)}, f_6^{(5)}, f_7^{(5)}) = TD\_PSD(LH\,2_v)$
$(f_1^{(6)}, f_2^{(6)}, f_3^{(6)}, f_4^{(6)}, f_5^{(6)}, f_6^{(6)}, f_7^{(6)}) = TD\_PSD(HL\,2_v)$
$(f_1^{(7)}, f_2^{(7)}, f_3^{(7)}, f_4^{(7)}, f_5^{(7)}, f_6^{(7)}, f_7^{(7)}) = TD\_PSD(HH\,2_v)$
$F_{49x1} = f_j^{(i)}, \quad i = 1, 2, \ldots, 7; \quad j = 1, 2, \ldots, 7$

- *Feature extraction using Gray Level co-occurrence matrix (GLCM)*

The GLCM is the feature that is used to identify texture in an image by modelling the surface as a 2-dimensional array of grey level variation. This array is called the grey-level co-occurrence matrix. GLCM is a statistical method that considers the spatial relationship of pixels; hence, it is also known as the grey-level spatial dependence matrix. [30, 41]. However, GLCM has been applied for feature extraction purposes in image detection [42, 43, 44]. The algorithm of Gray Level Co-occurrence Matrix is shown in algorithm 3.

Algorithm 3: Algorithm of Gray Level Co-occurrence Matrix [31,32**]**

Step 1- Convert the input image to grayscale
- Normalize the pixel values to a specific range

Step 2- Set the following parameters (Distance (d),:Angle (θ),
number of Gray Levels G)
Step 3.- Create GLCM Matrix-:
Initialize a *G x G* matrix, where each element (*i*, *j*)
represents the frequency of co-occurrence of gray levels
i and *j* at the specified distance and angle.
Step 4- Iterate through the image, with pixel and its neighboring
pixel at the specified distance and angle. Increment the corresponding
element in the GLCM matrix.
Step 5- Normalize the GLCM matrix by dividing each element by the total
number of pixel pairs considered.
Step 6.- Calculate various texture features from the GLCM matrix, {Contrast:
Correlation: Energy: Homogeneity: Entropy}

- *Fusion of selected features*

The term fusion is a process of combining information from more than one source in recognition process. Fusion helps in getting much more information from each biometric modality [47]. Fusion at the feature extraction level involves combining features extracted from multiple sources, such as sensors, modalities or algorithms to create a more comprehensive and robust feature set [45, 46]. The optimum features generated by MCSO from the normalized features from DWT (f_{dwt}), GLCM (f_{glcm}) and Gabor filter (f_{gabor}) were combined using the serial rule as shown in Equation 12.

$$F_f = \left\{F_{dwt}^{\varphi'}(t), F_{glcm}^{\varphi'}(t), F_{gabor}^{\varphi'}(t)\right\} \quad (12)$$

Where $F_{dwt}^{\varphi'}(t), F_{glcm}^{\varphi'}(t)$an $F_{gabor}^{\varphi'}(t)$ are the optimal normalized features from DWT, GLCM and Gabor

ISSN No:-2456-2165 https://doi.org/10.38124/ijisrt/25mar2010

techniques respectively. Algorithm 4 shows a simplified pseudocode for Serial Sum Fusion technique.

Algorithm 4: Serial Sum Fusion Pseudocode

Input {n: number of normalized features, x_i`: normalized features' values
w_i: weights for each normalized features}
Output
y: Fused output value
Procedure
1. Initialize y to 0.
2. For i from 1 to n:
   1. Calculate `weighted_value = $w_i$ * x_i`.
   2. Add weighted_value to y.
3. Return y as the fused output value.

➢ *The Simulated Binary Crossover*

The Simulated Binary Crossover (SBX) algorithm is a crossover operator used in genetic algorithms to combine two parent solutions and produce two offspring solutions. SBX is a simple and efficient crossover operator. It can be used for both continuous and discrete optimization problems. And it can produce offspring solutions that are significantly different from the parent solutions [54]. Here's a step-by-step explanation of the SBX algorithm:

Algorithm 5: SBX algorithm [54]

Step 1.- Initialization:
Initialize the parent solutions, ***`parent1`*** and ***`parent2`***, and
n: the number of variables / dimensions in the solution,
Step 2- . Distribution Index
: Set the distribution index, ***`eta_c`***, between 1 and 5.
Step 3.- Loop through variables
: Loop through each variable/ dimension in the solution, `i = 1` to `n`.
Step 4.- Generate a random number, ***`u`***, between 0 and 1.
Step 5 -. Spread Factor Calculation:
If $u \leq \frac{1}{(eta_c + 1)}$ then
$$beta = \left(2 * u(eta_c + 1)\right)^{\frac{1}{eta_c + 1}}$$
Else $$beta = \left(\frac{1}{2 * (1-u) * (eta_c + 1)}\right)^{\frac{1}{eta_c + 1}}$$
Step 6.
$$offspring1[i] = 0.5 * \{(1 + beta) * parent1[i] + (1 - beta) * parent2[i]\}$$
$$offspring2[i] = 0.5 * \{(1 - beta) * parent1[i] + (1 + beta) * parent2[i]\}$$
Step 7-. Repeat steps 4-6 .
Step 8-. Return the two offspring solutions, `offspring1` and `offspring2`.

➢ *Modification of Chicken Swarm Optimisation (mCSO)*

Chicken Swarm Optimisation (CSO) is a new bio-inspired algorithm developed by [48] for optimisation applications. It imitated the hierarchal order in the chicken swarm or shows the behaviors of the chicken swarm. The CSO algorithm has excellent research potential because of its good convergence speed and convergence accuracy. CSO can efficiently extract the chickens' swarm intelligence to optimize problems [49, 50] proposed an automatic framework for brain tumour detection in MRI. For more information [51, 52, 53].

In a simulated binary crossover based on CSO, two hens with the best fitness values are selected to do the crossover operation. Two chicks (child individuals) $x_{c1} = \{x_{c1}^1, \dots, x_{c1}^i, \dots, x_{c1}^n\}$ and $x_{c2} = \{x_{c2}^1, \dots, x_{c2}^i, \dots, x_{c2}^n\}$ are generated by a pair of parents (hens) with the best fitness $x_{p1} = \{x_{p1}^1, \dots, x_{p1}^i, \dots, x_{p1}^n\}$ and $x_{p2} = \{x_{p2}^1, \dots, x_{p2}^i, \dots, x_{p2}^n\}$ as follows in Equations 13 and 14.

$$x_{c1}^i = \frac{1}{2}\left[(1-\beta)x_{p1}^i + (1+\beta)x_{p2}^i\right] \quad (13)$$

$$x_{c2}^i = \frac{1}{2}\left[(1+\beta)x_{p1}^i + (1-\beta)x_{p2}^i\right] \quad (14)$$

β is generated in the following manner as in Equation 15:

$$\beta = \begin{cases} (2u)^{1/(\eta_c+1)} & if\ u \leq 0.5, \\ \left(\frac{1}{2(1-u)}\right)^{1/(\eta_c+1)}, & others \end{cases} \quad (15)$$

Where u is a random number in the range [0, 1]. η_c is the distribution index for the crossover operator. After the crossover operation, the two new offspring were taken the place of the two hens with the lowest fitness values, and the iterative process continues with other chickens. With the simulated binary crossover operator, the mCSO algorithm can modify the chickens' location while trapped in the local optimum. Therefore, the fitness values of the new offspring were better than those of roosters at a certain probability. With the mechanism of hierarchical order change in the CSO algorithm, the roosters were replaced by hens with better fitness values. This mechanism substituted the roosters that may be trapped in the local optimum and improve the search speed. Ultimately, the roosters have a faster speed towards the global optimum, accelerating the convergence rate.

Algorithm 5: Chicken Swarm Optimisation Algorithm.

Input:
`X`: Fused Brain tumor dataset with `n` samples and `F` Fused features
`y`: Class labels for the brain tumor dataset
`N`: Population size for the chicken swarm
`num_iterations`: Number of iterations for the mCSO algorithm

ISSN No:-2456-2165 https://doi.org/10.38124/ijisrt/25mar2010

`num_features`: Number of fused features to select

Output:

`selected_fusedfeatures`: Indexes of the selected fused features;

Define objective function $F(X) = \sum(w_i * g_i(X)) + p * \sum(h_j(X))$

where: - X is the position of the chicken;

- w_i are the weights for each objective function; - $g_i(X)$ are the objective functions,

- p is the penalty coefficient; - $h_j(X)$ are the constraint functions

Step 1: Initialization

1. Initialize the chicken swarm population with ` *N* ` chickens, each representing a random subset of features.

Initialize a population of *N* chickens by

$x_{I,J} = lb + Rand\ (ub - lb)$

with *lb* and *ub* are lower bound and upper bound of the search space

2. Set fitness $(f(x)) = {}^{1}/_{(1 + F(x))}$

where: - X is the position of the chicken, - F(X) is the objective function value

3. While (t < Max_Generation)

4. Evaluate the global best solution

***For** i = 1 to N*

$x_{i,j}(*) = x_{i,j} + S1 * Rand * (x_{l,j} - x_{i,j}) + S2 * Rand * (x_{n,j} - x_{i,j})$

$$S1 = exp\left(\frac{f_1 - f_{r1}}{abs(f_1) + \varepsilon}\right), \qquad s2 = exp(f_{r2} - f_1)$$

$x_i \neq x_l \neq x_n$

f is the fitness value of the corresponding *x*, *Rand* is a uniform random number over [0, 1], r1ϵ[1,..N] is an index of the rooster, which is the *i*th hen's group-mate, while r2ϵ[1,..N] is an index of the chicken (rooster or hen), which is randomly chosen from the swarm r1 ≠ r2.

If $fx_{i,j}(*) > f(x)$ then

$fx_{i,j}(*) = x_{i,j}(g)$ (individual global population)

5. Evaluate two local optimum solutions

First local optimum: $x_{i,j}(**) = x_{i,j}(g)\ Rand * (1 + Randn(0, \sigma^2))$ *with*

$$\sigma^2 = \begin{cases} 1 & f_i \leq f_i(g) \\ exp\left\{\frac{f_{ll(g)} - f_1(g)}{|f_1(g)| + \epsilon}\right\} & otherwise \end{cases}$$

$^{l}\epsilon[1,\ldots,N](g),\ I \neq i$

If $f x_{i,j}(**) > f x_{i,j}(g)$ then

$x_{i,j}(**) = x_{i,j}(\boldsymbol{l_1})$ (first local population)

Second local optimum: $x_{i,j}(***) = x_{i,j}(l_1) + C * (x_{n,j}(l_1) - x_{i,j}(l_1)),$

$x_n \epsilon[1,\ldots,N];\ x_n \neq x_i$ *and* $C\ \epsilon\ (0,2)$. is a parameter.

If $f x_{i,j}(***) > x_{i,j}(\boldsymbol{l_1})$ then

$x_{i,j}(***) = x_{i,j}(\boldsymbol{l_2})$ (second local population)

Apply SBX crossover operator to produce offspring solution

Step 1.- Set rooster1 = ***parent1***` and rooster2 = `***parent2***`, an ***n***: the number of variables / dimensions in the solution,

Step 2- . Set the distribution index, `$\eta_c$`, between 1 and 5.

Step 3.- Loop through each variable in the solution, `i = 1` to `n`.

Step 4.- Generate a random number, `***u***`, between 0 and 1.

Step 5 -. Factor Calculation:

$$\boldsymbol{\beta} = \begin{cases} (2u)^{1/(\eta_c+1)} & \boldsymbol{if\ u \leq 0.5,} \\ \left(\frac{1}{2(1-u)}\right)^{1/(\eta_c+1)}, & \boldsymbol{others} \end{cases}$$

Step 6. Estimate

$$x_{c1}^{i} = \frac{1}{2}\left[(1-\beta)x_{p1}^{i} + (1+\beta)x_{p2}^{i}\right]$$

$$x_{c2}^{i} = \frac{1}{2}\left[(1+\beta)x_{p1}^{i} + (1-\beta)x_{p2}^{i}\right]$$

Step 7-. Repeat steps 4-6

Set x_{c1}^{i}` = $f.\ x_{i,j}(\boldsymbol{l_1})$ and `$x_{c2}^{i} = f.x_{i,j}(\boldsymbol{l_2})$.

End For

2. Update the chicken's position :

If (fitness(x_i) ≥ fitness(x_{i-1})) then

Position Update

$x_i(t+1) = x_i(t) + v_i(t)$

Else

Velocity Update

$V_i(t+1) = w * V_i(t) + c_1 * r_1 * (x_{i,j}(\boldsymbol{l_2}) - X_i(t)) + c_2 * r_2 * (x_{i,j}(g) - X_i(t))$

Update the global best chicken and its fitness value if a better solution is found.

$Xi_{gbest}(t+1) = argmin(f(X(t+1)), f(Xi_{gbest}(t)))$ *for i = 1, 2, ..., N*

$x(t+1)_{pbest} = argMin\big(f(xi(t+1))\big), f(x_{pbesti}(t))\big)$

break

Step 3: Feature Selection

Set fusedfeature(i) = $X_{gbest}(i)$

Return (X_{pbest}, X_{gbest})

Next i

End While

➢ *Classification using SVM*

SVM was used in this work to classify features that was fused from extracted features. A multiple binary classification problem was explored to achieve a multiclass classification for four classes. Textural brain features were classified into Non tumour and tumour. SVM classification predictions for the best hyperplane with the maximum margin was achieved using Equation 16 to make.

$$g(x) = w^T x + w_0 = 0 \tag{16}$$

ISSN No:-2456-2165 https://doi.org/10.38124/ijisrt/25mar2010

Where x is the feature descriptor and w and w_0 are unknown parameters, derived from training samples $\{(x_i, y_i)|1 \leq i \leq N\}$ (xi, yi) where $y_i \in \{+1, -1\}$is the class label. The calculation entails the solution of an optimization problem based on big margin theory. After computing the best hyperplane, Equation 17 were used to classify a test sample x.

$$g(x) = \sum_{i=1}^{N_s} \lambda_i y_i x_i^T x + w_0 \quad (17)$$

Where λ_i are Lagrange multipliers and N_s is the number of support vectors i.e., the training samples corresponding to non-zero λ_i. The Kernel technique is employed when the data samples from two classes are not linearly separable. The function g(x) is represented as Equation 18 using a kernel function.

$$g(x) = \sum_{i=1}^{N_s} \lambda_i y_i K(x_i, x) + w_0 \quad (18)$$

Where $K(x_i, x)$ is the kernel function that expresses the data's inner product. The user-defined parameter C in the higher-dimensional space were utilized to regulate the misclassified penalty. The misclassification penalty or error is related to the kernel and adjusted by a user-defined parameter C. The RBF kernel was utilized in this work, as shown in Equation 19 with *C* set to 2000.

$$K(x_i, x) = \exp(-\gamma \|x_i - x\|^2), \gamma > 0 \quad (19)$$

The width of the kernel function is the γ. The RBF kernel now has two parameters γ and *C*.

➢ *Performance Evaluation Measures*

The effectiveness of the analysed techniques was assessed by evaluating their recognition accuracy, False Positive Rate (FPR), precision, sensitivity, and computation time. These performance metrics were calculated using a confusion matrix, defined in Equations 20 to 23, which includes True Positive (TP), False Positive (FP) and True Negative (TN).

$$\text{False Positive Rate (FPR)} = \frac{\text{FP}}{\text{TN+FP}} \quad (20)$$

$$\text{Sensitivity} = \frac{\text{TP}}{\text{TP+FN}} \quad (21)$$

$$\text{Precision} = \frac{\text{TP}}{\text{TP+FP}} \quad (22)$$

$$\text{Accuracy} = \frac{\text{TP+TN}}{\text{TP+TN+FP+FN}} \quad (23)$$

IV. RESULTS AND DISCUSSION

The techniques considered in this work were implemented using MATLAB R2018a on a computer system with suitable processor speed, memory, and operating system. The application was designed to run across different platforms. Figure 5 depicts the graphical user interface of the developed system. The evaluation of the performance of the fusion of three extracted textual features without CSO (noCSO), with standard CSO (CSOst) and with modified CSO (mCSO) in detection/classifying is presented. The developed system was evaluated at different threshold values of 0.25, 0.45, 0.65 and 0.85. across all the developed techniques. The acquired dataset comprised of 1800 brain MRI images from the Kaggle database. In this study, multiclass classification schemes were considered to ascertain the effectiveness of each feature selection technique.

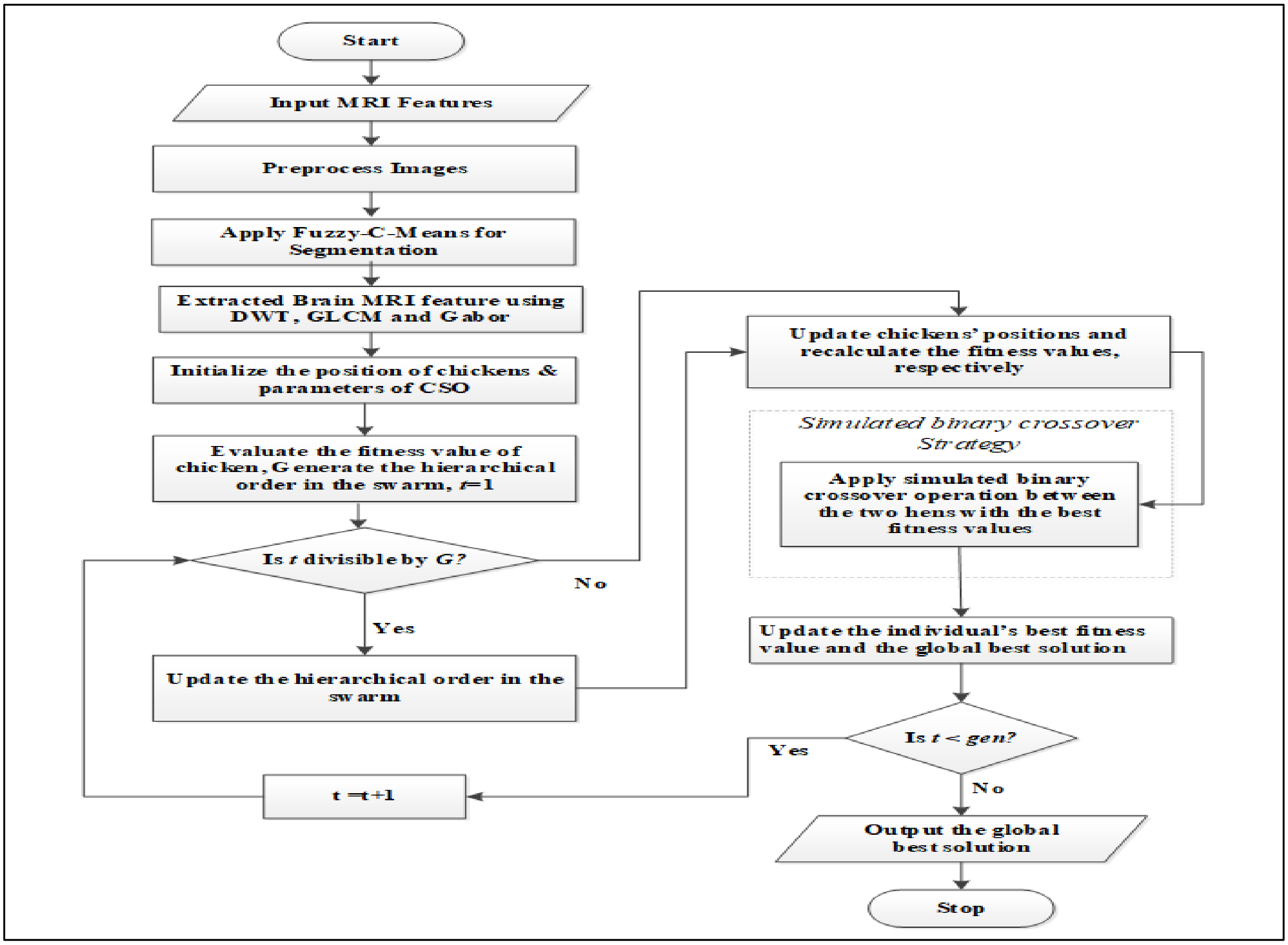

Fig 4 Flowchart of the Developed System

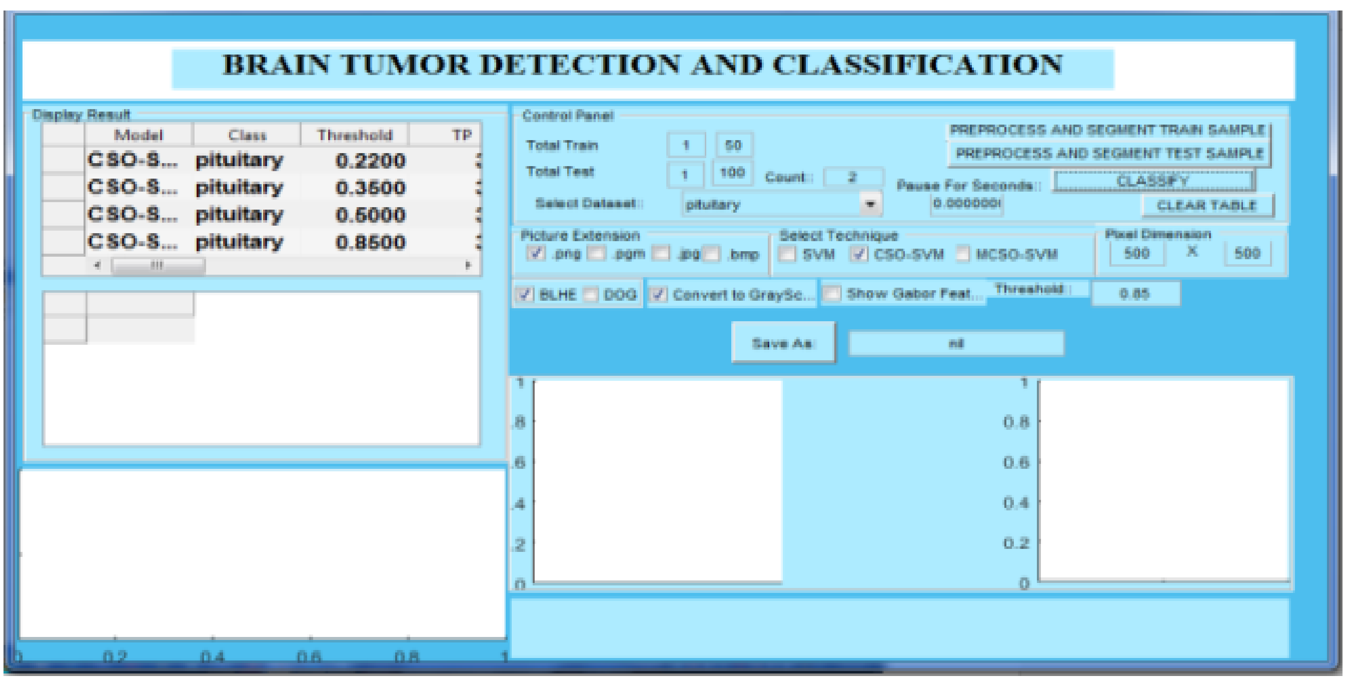

Fig 5 Graphical User Interface of the Developed System

ISSN No:-2456-2165 https://doi.org/10.38124/ijisrt/25mar2010

A series of pre-processing steps were applied to improve the image quality for further processing Figures 6, 7, 8 and 9 illustrate the pre-processing stages. The acquired images were passed through different pre-processing techniques, and the MRI brain images were resized to equal pixels and converted to a grey-level image.

Aquired image	Image resizes	Gray scale	Filter image	Segmentation	Contrast adjustment

Fig 6 The Pre-Processed Glioma

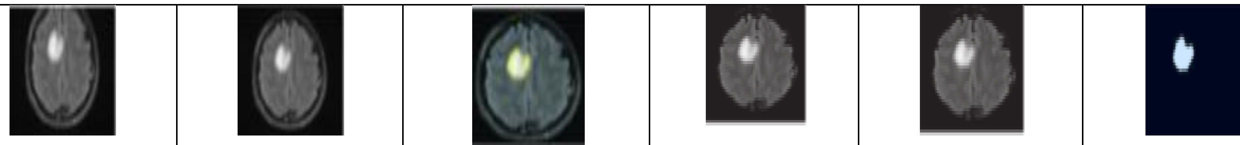

Aquired image	Image resizes	Gray scale	Filter image	Segment-ation	Contrast adjustment

Fig 7 The Pre-processed meningioma

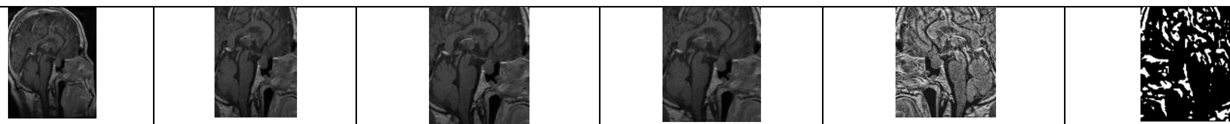

Aquired image	Image resizes	Gray scale	Filter image	Segmen-tation	Contrast adjustment

Fig 8 The Pre-processed pituitary

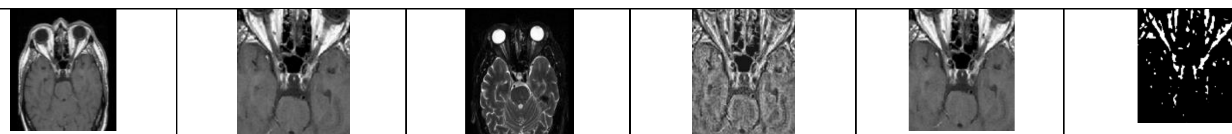

Aquired image	Image resizes	Gray scale	Filter image	Segmen-tation	Contrast adjustment

Fig 9 The Pre-Processed Non Tumour

The results in Tables 1 and 2 show how well the fused three textural features worked with noCSO, CSOst and mCSO on brain tumour images. From Table 1 shows the results of noCSO feature selection on brain tumour detection system. At the threshold of 0.85, the noCSO system produced 1369, 332, 48, 51, 96.42%, 87.44%, 12.62%, 94.51%, 96.58%, 166.47msec for TP, TN, FP, FN, Recall, Specificity, FPR, Accuracy, Precision and Computation time respectively. From Table 2, at the threshold of 0.85, the CSOst system produced 1387, 350,30,33, 97.74%, 92.06%, 7.85%, 96.52%. 97.88%, 157.92msec for TP, TN, FP, FN, Recall, Specificity, FPR, Accuracy, Precision and Computation time respectively. From Table 3, at the threshold of 0.85, the MCSO system produced 1397, 360, 20, 23, 98.41%, 94.68%, 5.26%,97.63%, 98.61%, 119.82msec for TP, TN, FP, FN, Recall, Specificity, FPR, Accuracy, Precision and Computation Time respectively. The graphs representation of the results are shown in figures 10, 11,12 and 13.

Table 1 Performance Evaluation of noCSO Tumour Detection System on Fused Three Textural Features

Thres.	**TP**	**TN**	**FP**	**FN**	**REC%**	**SPEC%**	**FPR%**	**ACC%**	**PREC%**	**CT(μsec)**
0.25	1288	295	109	108	92,22	73.04	27.01	87.88	92.14	162.22
0.45	1309	301	97	93	93.39	75.55	24.38	89.44	93.07	163.23
0.65	1331	311	77	81	94.31	80.24	19.93	91.19	94.49	164.06
0.85	1369	332	48	51	96.42	87.44	12.62	94.51	96.58	166.47

ISSN No:-2456-2165 https://doi.org/10.38124/ijisrt/25mar2010

Table 2 Performance Evaluation of CSOst Tumour Detection System on Fused Three Textural Features

Thres.	**TP**	**TN**	**FP**	**FN**	**REC%**	**SPEC%**	**FPR%**	**ACC%**	**PREC%**	**CT (µsec)**
0.25	1319	317	83	81	94,21	79.32	20.78	90.89	94.03	157.27
0.45	1337	324	66	73	94.83	83.14	16.91	92.26	95.32	157.31
0.65	1355	339	58	48	96.62	85.44	14.57	94.09	95.86	157.43
0.85	1387	350	30	33	97.74	92.06	7.85	96.52	97.88	157.92

Table 3 Performance Evaluation of m CSO Tumour Detection System on Fused Three Textural Features

Thres.	**TP**	**TN**	**FP**	**FN**	**REC%**	**SPEC%**	**FPR%**	**ACC%**	**PREC%**	**CT (sec)**
0.25	1341	322	66	71	94.85	82.89	17.04	92.42	95.31	119.74
0.45	1358	328	54	60	95.75	85.85	14.03	93.66	96.24	119.79
0.65	1371	349	32	48	96.58	91.59	8.37	95.57	97.65	119.80
0.85	1397	360	20	23	98.41	94.68	5.26	97.63	98.61	119.82

Table 4 Comparison of the Results with Existing Systems

Features Extraction Method	**Classifier**	**Accuracy (%)**	**Author**
DWT + Gabor Filter	Artificial Neural Network	91.9	Ismaila et al. (2018)
Genetic Algorithm	Support Vector Machine	> 90	Sharif et al. (2018)
Gabor + DWT +GLCM/mCSO	Support Vector Machine	97.61	Developed Technique

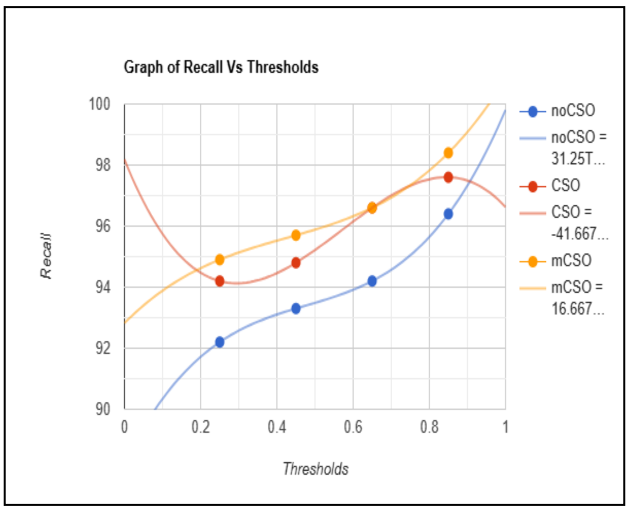

Fig 10 ROC curves of Sensitivity and Thresholds

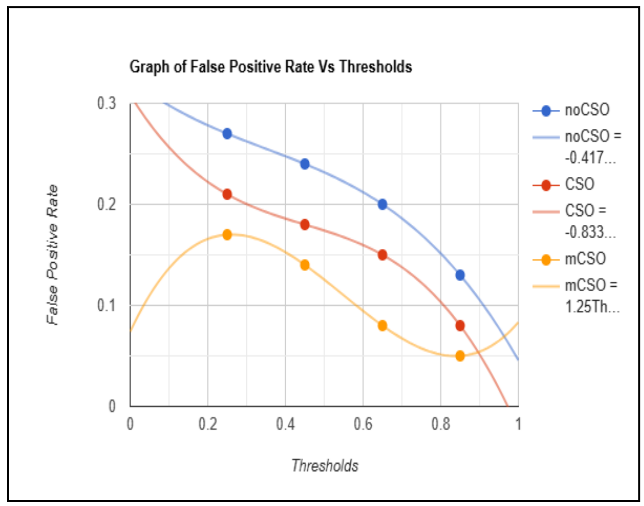

Fig 12 ROC curves of FPR and Thresholds

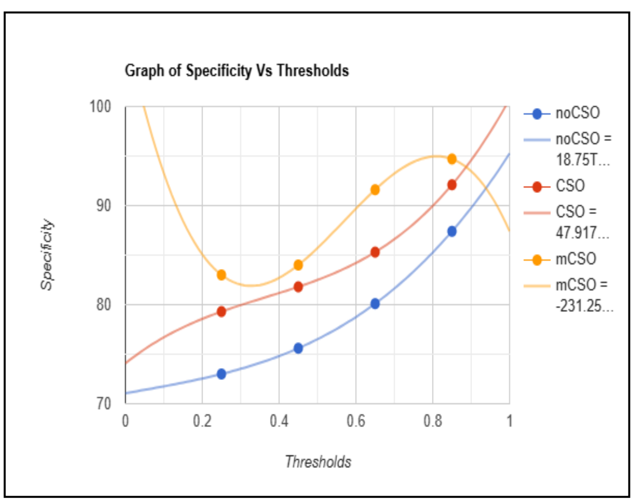

Fig 11 ROC curves of Specificity and Thresholds

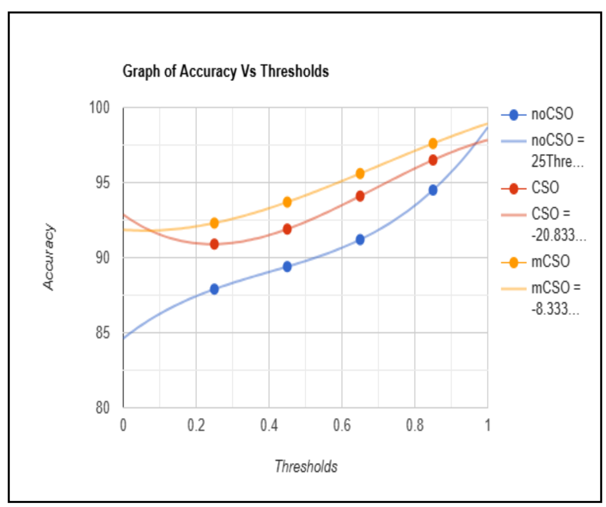

Fig 13 ROC curves of Accuracy and Thresholds

ISSN No:-2456-2165 https://doi.org/10.38124/ijisrt/25mar2010

V. CONCLUSION

This research developed an mCSO for feature selection optimisation in the classification and detection of brain tumour images. The research investigated and improved the capability of CSO for feature selection by developing a mCSO to achieve the selection of relevant features and better classification performance. The Kaggle database repository was used in the evaluation of the developed technique. The performance of the developed mCSO technique was evaluated using false positive rate, sensitivity, precision, accuracy, and computation time. This study developed a modified CSO by adding a simulated binary crossover operator to the CSOst method which reduced problem of local optima or convergent too soon. Also, the t-test statistical analysis, mCSO was adjudged a better algorithm when compared with CSO standard technique in the detection and classification of tumour images using the most significant and balanced brain tumour image features .

ACKNOWLEDGEMENT

I appreciate TETFUND for her financial support toward the successful completion of this research.

REFERENCES

[1]. Zhang J., Hsu W., Mong L. L. (2001). Image Mining: Issues, Frameworks and Techniques, Proceedings of the Second International workshop on Multimedia Data Mining (MDM/KDD2001), in conjunction with ACM SIGFDD Conference, USA. 13-20.

[2]. Shree N. V. and Kumar T. N. R. (2018). Identification and classification of brain tumour MRI images with feature extraction using DWT and probabilistic neural network. Brain Informatics (2018) 5:23–30.

[3]. Pagadala P. K., Omkari D Y., Lakshmi P S, Dewi C. , Sutresno S. A., Christanto H. J. (2024). Automated Brain Tumour Detection With GLCM Based Feature Extraction And PCA For Dimension Reduction And Classification Using Machine Learning, Journal of Theoretical and Applied Information Technology, 102(12).

[4]. Abudu S. D., Inuwa I., Adedoyin A. A.and Kolo, S. S. (2019). "Automated Brain Tumour Detection using PCA and SVM Classifier," Journal of Medical Systems, 43(6), 148.

[5]. Nabizadeh, N. and Kubat, M. (2015) Brain tumours detection and segmentation in MR images: Gabor wavelet vs. statistical features. *Computers & Electrical Engineering*, *45*, 286-301.

[6]. Mathew, A. R., Anto, P. B., and Thara, N. K. (2017). Brain Tumour Segmentation and Classification using DWT, Gabour Wavelet and GLCM. *2017 International Conference on Intelligent Computing, Instrumentation and Control Technologies (ICICICT)*, 1744-1750.

[7]. Ismael, M.R. , and Abdel-Qader, I. (2018). Brain Tumor Classification via Statistical Features and Back-Propagation Neural Network *The Institute of Electrical and Electronics Engineers (IEEE)*, 0252 – 0257.

[8]. Sharif, M., Tanvir, U., Munir, E. U., Khan, M. A., and Yasmin, M. (2018). Brain Tumour Segmentation and Classification by Improved Binomial Thresholding and Multi-Features Selection. *Journal of Ambient Intelligence and Humanized Computing*, 1-20.

[9]. Dandu J. R., Thiyagarajan A. P., Murugan P. R.,Govindaraj V. (2019) Brain and pancreatic tumour segmentation using SRM and BPNN classification. Health Technol:1–9.

[10]. Ramkumar, M., Babu, M., and Lakshminarayanan, R.(2019). Classification of Brain Tumor using Bees Swarm Optimisation. *ICTACT Journal on Image and Video Processing*, **10**(1), 2025-2030.

[11]. Meng, X. , Liu, Y. , Zhang, H. , and Gao, X (2014).*A New Bio-Inspired Algorithm: Chicken Swarm Optimization," in Advances in Swarm Intelligence.* Paper presented at the International conference in swarm intelligence. Springer, Cham,

[12]. Al Shayokh, M., and Shin, S.Y. (2017). Bio Inspired Distributed WSN Localization Based on Chicken Swarm Optimization. *Wireless Personal Communications*, **97**(4), 5691-5706.

[13]. Zhenwu, W. , and Chengfeng, Y. (2018). Chicken Swarm Optimization Algorithm Based on Behavior Feedback and Logic Reversal *Journal of Beijing Institute of Technology*, **27**(3), 348-356.

[14]. Sathi, K.A. , and Islam, M.S. (2020). Hybrid Feature Extraction Based Brain Tumor Classification using an Artificial Neural Network. *IEEE 5th International Conference on Computing Communication and Automation (ICCCA), 2020*, 155-160.

[15]. Damodharan, S., and Raghavan, D. (2015). Combining Tissue Segmentation and Neural Network For Brain Tumour Detection. *International Arab Journal of Information Technology*, *12*(1), 42 52.

[16]. Alias, N., Alwesabi, Y., and Mugahed Al-Rahmi, W. (2017). Chronology of Brain Tumour Classification of Intelligent Systems Based on Mathematical Modeling, Simulation and Image Processing Techniques. *Journal of Theoretical and Applied Information Technology*, *95*(19), 4949‒4963.

[17]. Siddiqui, M., Mujtaba, G., Reza, A., and Shuib, L. (2017). Multi-Class Disease Classification in Brain MRIs Using a Computer-Aided Diagnostic System. *Symmetry*, *9*(3), 37.

[18]. Minz, A., and Mahobiya, C. (2017, 2017/01). *MR Image Classification Using Adaboost for Brain*

ISSN No:-2456-2165 https://doi.org/10.38124/ijisrt/25mar2010

Tumour Type 2017 IEEE 7th International Advance Computing Conference (IACC),

[19]. Gumaei, A. H., Hassan, M. M., Hassan, M. R., Alelaiwi, A., and Fortino, G. (2019). A Hybrid Feature Extraction Method with Regularized Extreme Learning Machine for Brain Tumour Classification. *Journal of Insittue of Electrical and Electronic Enginer Access 7*, 36266-36273.

[20]. Mohammadi, F. G., Amini, M. H., and Arabnia, H.R. (2020). Applications of Nature-Inspired Algorithms for Dimension Reduction: Enabling Efficient Data Analytics. In *Advances in Intelligent Systems and Computing* (67-84).

[21]. Ghosh, K. K., Guha, R., Bera, S. K., Sarkar, R., and Mirjalili, S. (2020). BEO: Binary Equilibrium Optimizer Combined with Simulated Annealing for Feature Selection. In: Research Square Platform LLC.

[22]. Prabhakar, S. K., Rajaguru, H., and Won, D. (2021). A Holistic Performance Comparison for Lung Cancer Classification Using Swarm Intelligence Techniques. *Journal of healthcare engineering, 2021*, 6680424-6680424.

[23]. Ismaila, W. O., Babalola, O. R., Ismaila, F. M., and Ogunjimi, T. O. (2018). Soft Computing: Two-Step Feature Extraction-Based Biometric Authentication System. *International Journal of Emerging Technologies in Computational and Applied Sciences, 25*(1), 22-27.

[24]. Johnson, S. B., Blum, R. W., and Giedd, J. N. (2009). Adolescent Maturity and the Brain: The Promise and Pitfalls of Neuroscience Research in Adolescent Health Policy. *The Journal of adolescent health : official publiation of the Society for Adolescent Medicine, 45*(3), 216-221.

[25]. Lahmiri, S., and Boukadoum, M. (2013). Hybrid Discrete Wavelet Transform and Gabor Filter Banks Processing for Features Extraction from Biomedical mages. *Journal of Medical Engineering, 2013*, 1–13.

[26]. Taghavirashidizadeh A., Sharifi F., Vahabi S. A., Hejazi A., Torbati M., Mohammed A. S., (2022). WTD-PSD: Presentation of Novel Feature Extraction Method Based on Discrete Wavelet Transformation and Time-Dependent Power Spectrum Descriptors for Diagnosis of Alzheimer's Disease, Hindawi, Computational Intelligence and Neuroscience, Vol.2022.

[27]. Manjunath, B. S., and Chellappa, R. (1991). Unsupervised texture segmentation using Gabor filters. Proceedings of the IEEE Conference on Computer Vision and Pattern Recognition, 14-19.

[28]. Fogel, I., and Sagi, D. (1989). Gabor filters as texture discriminator. Biological Cybernetics, 61(2), 103-113.

[29]. Mallat, S. G. (1989). A theory for multiresolution signal decomposition: The wavelet representation. IEEE Transactions on Pattern Analysis and Machine Intelligence, 11(7), 674-693.

[30]. Daubechies, I. (1992). Ten lectures on wavelets. Society for Industrial and Applied Mathematics.

[31]. Mohanaiah, P., Sathyanarayana, P., and GuruKumar, L. (2013). Image Texture Feature Extraction Using GLCM Approach. *International Journal of Scientific and Research Publications*, **3**(5), 1-5.

[32]. Soh, L.-K., and Tsatsoulis, C. (1999). Texture analysis of SAR sea ice imagery using gray level co-occurrence matrices. IEEE Transactions on Geoscience and Remote Sensing, 37(2), 780-795.

[33]. Vironicka A S. and Sathiaseelan J. (2022). Texture Feature Extraction with Medical Image Using GLCM and Machine Learning Techniques, ICTACT Journal on Image and Video Processing, 12(04): 2735- 2740.

[34]. Lee, T.S. . (1996). Image Representation Using 2d Gabor Wavelets. *Institue of Electrical and Electronic Engineering Transactions on Pattern Analysis and Machine Intelligence*, **18**(10), 959–971.

[35]. Fouad, A., Moftah, H.M., and Hefny, H.A. (2019). MRI Brain Cancer Diagnosis Approach Using Gabor Filter and Support Vector Machine. *International Journal of Emerging Trends in Engineering Research*, **7**(12), 907-914.

[36]. Hao, Y., Zhang, L. , and Zhang, D. . (2017). The Fusion of Gabor Feature and Sparse Representation for Face Recognition. *Journal of computers*, **28**(2), 1991-1599.

[37]. Li, W., Mao, K., Zhang, H., and Chai, T. (2010). *Selection of Gabor Filters for Improved Texture Feature Extraction*. Paper presented at the Proceedings of 2010 IEEE 17th International Conference on Image Processing, Hong Kong.

[38]. Kong, W.K., Zhang, D., and Li, W. (2003). Palmprint Feature Extraction using 2-D Gabor Filters. *Pattern Recognition*, **36**(10), 2339-2347.

[39]. Percival, D.B., and Walden, A.T. (2000). The Discrete Wavelet Transform. In *Wavelet Methods for Time Series Analysis* (56-158): Cambridge University Press.

[40]. Yang, G., Nawaz, T., Barrick, T.R., Howe, F.A., and Slabaugh, G. (2015). Discrete Wavelet Transform-Based Whole-Spectral and Subspectral Analysis for Improved Brain Tumor Clustering Using Single Voxel MR Spectroscopy. *IEEE Transactions on Biomedical Engineering*, **62**, 2860-2866

[41]. He, Q., and Lin, D. (2011). Avariable Selection Method for Genome-wide Association Studies. *Bioinformatics*, **27**(1), 1–8.

[42]. Sastry, S.S., Kumari, T.V., Rao, C.N., Mallika, K., Lakshminarayana, S., and Tiong, H.S. (2012). Transition Temperatures of Thermotropic Liquid Crystals from the Local Binary Gray Level Cooccurrence Matrix. *Advances in Condensed Matter Physics*, 2012, 1-9

ISSN No:-2456-2165 https://doi.org/10.38124/ijisrt/25mar2010

[43]. Farhi, L., and Yusuf, A. (2017). *Comparison of Brain Tumor MRI Classification Methods Using Probabilistic Features*. Paper presented at the 13th IASTED International Conference on Biomedical Engineering (BioMed).

[44]. Lapointe, S., Perry, A., and Butowski, N.A. (2018). Primary Brain Tumours in Adults. *Lancet (London, England)*, 392(10145), 432–446

[45]. Haralick, R.M., Shanmugam, K., and Dinstein, I. . (1973). Textural Features for Image Classification. *IEEE Transactions on Systems, Man and Cybernetics*, **3**(6), 610–621.

[46]. Li, H., Liu, L., Huang, W., and Yue, C. (2016). An Improved Fusion Algorithm for Infrared and Visible Images Based on Multi-Scale Transform. *Infrared Physics and Technology*, **74**, 28–37.

[47]. Zhou, Y., Yu, L., Zhi, C., Huang, C., Wang, S., Zhu, M., Ke, Z., Gao, Z., Zhang, Y., and Fu, S. (2022). A Survey of Multi-Focus Image Fusion Methods. *Applied Sciences*, **12**, 6281.

[48]. Akansha, S., Hitakshi, G., and Yashika, S. (2021). Image Fusion with Deep Leaning using Wavelet Transformation *Journal of Emerging Technologies and Innovative Research*, **8**(3), 2826-2834.

[49]. Sireesha V., Sandhyaran K. (2014). International Journal of Engineering Research & Technology (IJERT) IJERT www.ijert.org NCDMA - 2014 Conference Proceedings. 3-6.

[50]. Meng, X. , Liu, Y. , Zhang, H. , and Gao, X (2014). *A New Bio-Inspired Algorithm: Chicken Swarm Optimization," in Advances in Swarm Intelligence.* Paper presented at the International conference in swarm intelligence. Springer, Cham

[51]. Cuevas, E., Cienfuegos, M., Zaldivar, D., and Cisneros, M. . (2013). A Swarm Optimization Algorithm Inspired in The Behavior of The Social-Spider. Expert Systems with Applications.40, 6374–6384.

[52]. Taie, S.A., and Ghonaim, W. . (2017, 13th - 17th March, 2017). *CSO-Based Algorithm with Support Vector Machine for Brain Tumor's Disease Diagnosis*. Paper presented at the 2017 IEEE International Conference on Pervasive Computing and Communications Workshops (PerCom Workshops), Kona, Big Island, HI, USA.

[53]. Cristin, D.R., Kumar, D.K.S., and Anbhazhagan, D.P. (2021). Severity Level Classification of Brain Tumor Based on MRI Images using Fractional-Chicken Swarm Optimization Algorithm. *The Computer Journal*, 64(10), 1514–1530

[54]. Deb, S., Gao, X.Z., Tammi, K., Kalita, K., and Mahanta, P. (2020). Recent Studies on Chicken Swarm Optimization Algorithm: A Review (2014–2018). *Artificial Intelligence Review*, 53(3), 1737-1765.

[55]. Marino, L. (2017). Thinking Chickens: A Review of Cognition, Emotion, and Behavior in the Domestic Chicken. *Animal Cognition*, **20**(2), 127-147.

[56]. Deb, K., and Agrawal, S. (1999). A niched-penalty approach for constraint handling in genetic algorithms. Proceedings of the International Conference on Artificial Neural Networks and Genetic Algorithms, 235-240.